Journal of Medicinal and Chemical Sciences 5 (2022) 1265-1280

Journal of Medicinal and Chemical Sciences

Journal homepage: http://www.jmchemsci.com/

Original Article (Special Issue)

Electrochemical Investigation of Poly Vinyl Alcohol-G-Succinic Acid Doped with Malachite Green

Samah Hussein Kadhim*

Department of Chemistry, College of Science, University of Thi-Qar, Iraq

ARTICLE INFO

Article history

Receive: 2022-05-19
Received in revised: 2022-06-28
Accepted: 2022-07-30
Manuscript ID: JMCS-2207-1586
Checked for Plagiarism: **Yes**
Language Editor:
Dr. Fatimah Ramezani
Editor who approved publication:
Prof. Dr. Hassan Karimi-Maleh

DOI:10.26655/JMCHEMSCI.2022.7.16

KEYWORDS

Cyclic voltammetry
Poly vinyl alcohol
Malachite green
Supporting electrolyte

ABSTRACT

The electrochemical manner was investigated for poly vinyl alcohol -g-succinic acid by using the cyclic voltammetry mechanism. Such an investigation mostly concentrates on the expected properties of the doped polymers with different doping ratios of Malachite green (0.03, 0.06, 0.09, 0.12, and 0.15) %wt. This is specific by the electrons transmit between the dopants and both polymers, which visibly show the appearance of oxidation-reduction peak accompanied log increase in electrical current Ip as applied potential changer. The heights of Ip oscillate due to the change in see rate ν. The results of linear of relationships between Ip and $\nu^{1/2}$specificed that the electron transfer was a process of one electron transfer

GRAPHICAL ABSTRACT

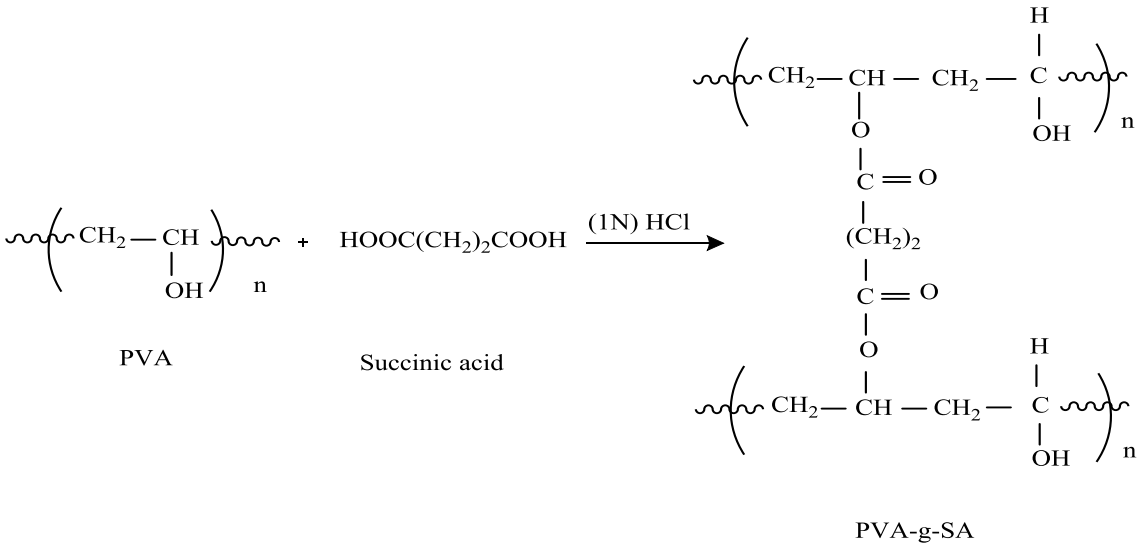

* Corresponding author: Samah Hussein Kadhim
✉ E-mail: Email: Samah.h_chem_chem@sci.utq.edu.iq

Introduction

Cyclic voltammetry is a very important electrochemical technique. It can be used to study the redox manner of compounds and probe coupled chemical reactions, in particular to determine mechanisms and rates of oxidation-reduction reactions.

The study of cyclic voltammetry with different scan rates offers much acquaintance about electron transfer, kinetics, and transport properties of electrolysis reaction. The current labor is considered as a function of the linear potential applied. Such a current divergence that results, when the electrode potential is numerous, can provide a valuable prudence into the reactions that occur at the electrode surface [1].

Cyclic voltammetry is a method for the electrochemical manner of a system. It was first reported in 1938 and described theoretically by Randles [2].

Cyclic voltammetry is the most vastly used technicality to acquire qualitative information about electrochemical reactions. The power of cyclic voltammetry results from its ability to rapidly provide considerable information on the thermodynamics of redox processes, on the kinetics of heterogeneous electron-transfer reactions, and uncoupled chemical reactions, or adsorption processes. Cyclic voltammetry is often the initial experimental approach performed in an electro analytical study, since it offers rapid location of redox potentials of the electro active species and convenient evaluation of the effect of media upon the redox [3-4].

The cyclic voltammetry (scanning in forward and back directions) and linear voltammetry (scanning in one direction) are the most widely used techniques to investigate electrode reaction mechanisms. They are easy to apply experimentally and readily available in commercial instruments, and also provide a wealth of mechanistic information. In such experiments, the potential of working electrode is controlled by a potential ramp or one or more potential triangle.

The peak current in a cyclic voltammogram containing only one species is described by Sevcik- Randles [5]:

$$I_P=(2.69x105)n^{3/2}AD^{1/2}v^{1/2}C^* \quad (1)$$

at 25 °C, where Ip is the peak current, n is the number of electrons transferred, A is the electrode area, D is the diffusion of species, v is the scan rate, and C* is the bulk concentration of species. If the diffusion constants for the oxidized and reduced species are similar, the E^o value (formal potential) can be estimated from the average of E_{pa} and E_{pc}, where E_{pa} is the potential of anodic peak current and $E_{pc}$is the potential of the cathodic current [6].

Cyclic voltammetry is a useful technique for probing the probing the processes that occur at the electrode-solution interface. This technique is not generally well understood in comparison to other instrumental methods such as spectroscopy and chromatography. It is not uncommon for the experimenter who is performing CV to have a poor understanding of the basic concepts of the technique, such as why the voltammograms have their peculiar shapes [7].

Materials and Methods

The materials tested in this study were polyvinyl alcohol, succinic acid, hydrochloric acid, and malachite green.

Preparation of poly vinyl alcohol copolymer succinic acid (PVA-g-SA)

In a round flask of 250 mL capacity, (13.328 g, 0.0136 mol) of polyvinyl alcohol (PVA) was put which dissolved in 70 mL distilled water, and then (1.6 g, 0.0136 mol) of succinic acid and 2 mL of 1N hydrochloric acid were added and the mixture was stirred at 70 °C for 8 hours [8], after the reaction was completed, we noticed the formation of white color polymer, and the yield was 82% (Scheme 1).

Doping of PVA-g-SA

Doping PVA-g-SA with dye malachite green was carried out by adding the weighted dye to the appropriate weight of polymer (1g), and then the mixture was dissolved in dimethyl formamide DMF after the prepared directly to give a

polymer/dye system containing (0.03, 0.06, 0.09, 0.12, and 0.15) g wt% of doping reagent malachite green [9]. The mixture was stirred well for 20 minutes to guarantee that the homogenous distribution of dye in the polymer matrix.

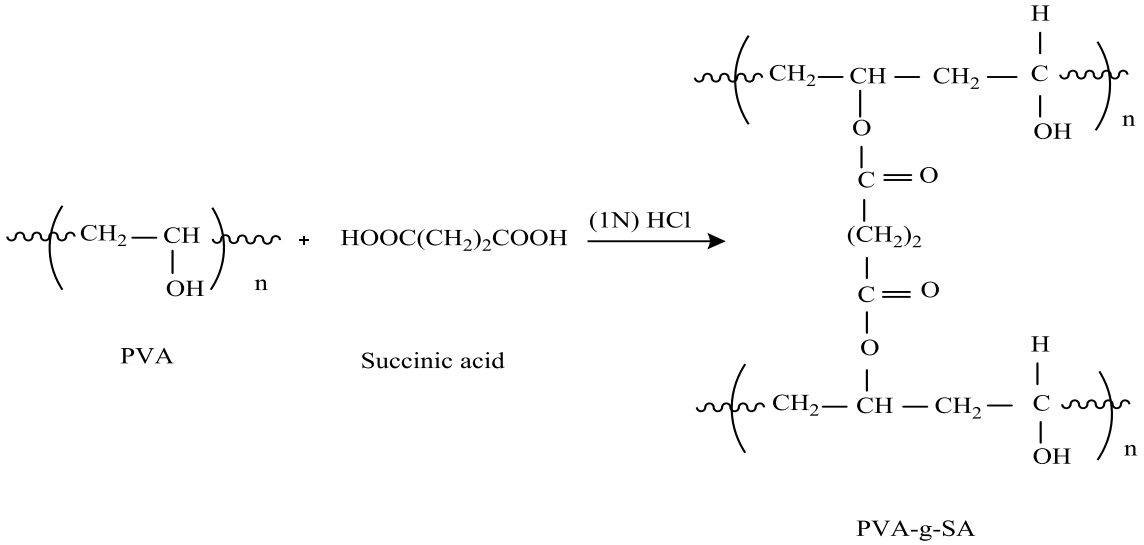

Scheme 1: Preparation of poly vinyl alcohol Graft succinic acid (PVA-g-SA)

Electrochemical measurements

Cyclic voltammetry (CV) was carried out in a thermo stated one compartment three -electrode cell. The working electrode was a platinum wire of nominal area 0.0785 cm^2. This was controlled by silver-silver chloride as a reference electrode through which no current flows. The auxiliary (secondary) electrode was a platinum wire. Cyclic voltammetry was performed with a DY 2300 Series Potentiostat/Bipotentiostat, potentiostate-galvanostate fully computerized in the processed data analysis.

In cyclic voltammetry (CV), the voltage is linearly varied from initial to final potential values as required, and then directly swept back at the same sweep rate to the initial one. The current response is plotted as a function of voltage rather than time. The species were reduced and oxidized in the manner of reversible reactions. During all measurements Bu_4NBF_4 was used as a supporting electrolyte.

In cyclic voltammetry, the negative initial potential value was set mostly equal to the final positive one. The scan rate (ν) was varied from 0.1 to1 Vs^{-1}, while the voltage was canned between -2 to 2V. The molar concentration of supporting electrolyte Bu_4NBF_4 was 0.15 M. The solutions of pure PVA-g-SA and the doped solutions with different weight ratios of malachite green (0.03, 0.06, 0.09, 0.12, and 0.15) wt% were all subjected to cyclic voltammogram, to achieve a comparison with the measured precursor cyclic voltamograms of pure solutions. All measurements were performed at room temperature.

Results and Discussion

The electrochemical behavior of the PVA-g-SA and its doping ratios were established by cyclic voltammetry (CV) for oxidation and reduction at a platinum electrode in DMF at scan rates that ranged from 0.1 to 1 Vs^{-1} at a potential range of 2 to -2V. At scan rate (ν) 0.05 Vs^{-1}, as an example, one reduction peak was clearly obtained for PVA-g-SA at Ep_{red1}=-0.8 V corresponding to the cathodic peak current $Ip_{red1}=1.2\times10^{-5}$A. At the same scan rate and potential range, the cyclic voltammogram shows also a oxidation peak at Ep_{ox1}=-0.82V corresponding to the cathodic peak current $Ip_{ox1}=1.5\times10^{-5}$ A, as displayed in Figure 1.

It is obvious that the reduction and oxidation peaks were shifted to more negative potential values as ν increases accompanied by an increase in the current peak. This behavior is indicated and confirmed by Sevcik-Randles Equation 1.

According to the same Equation 1, which presented the relationship between the peak current Ip and the square root of the scan rate

$\nu^{1/2}$, the following graphic relations are established:

$$Ip \& \nu^{1/2}$$

$$Fp \& \nu$$

Where, $Fp = Ip / \nu^{1/2}$ and it is known as current function. Thus, both Fp^{red} (reduction) and Fp^{ox} (oxidation) can be computed. Table (1) illustrates the obtained data for the reduction and oxidation states of the PVA-g-SA. Figure 2 represents a linear relationship between Ip_{red} and Ip_{ox} with $\nu^{1/2}$ of PVA-g-SA indicating that the electron transfer is a process of one electron transfer. Figure 3 shows the plot of Fp^{red} and Fp^{ox} vs. ν from which it is clear that the Fp^{red} and Fp^{ox} are essentially invariant with ν provided that $\nu > 0.1\ Vs^{-1}$ a condition which isolates the primary electron transfer from the subsequent chemical step. The Fp independence is a diagnostic signal of diffusion-controlled electron transfer at specified potentials beyond the peak potential [10,11].

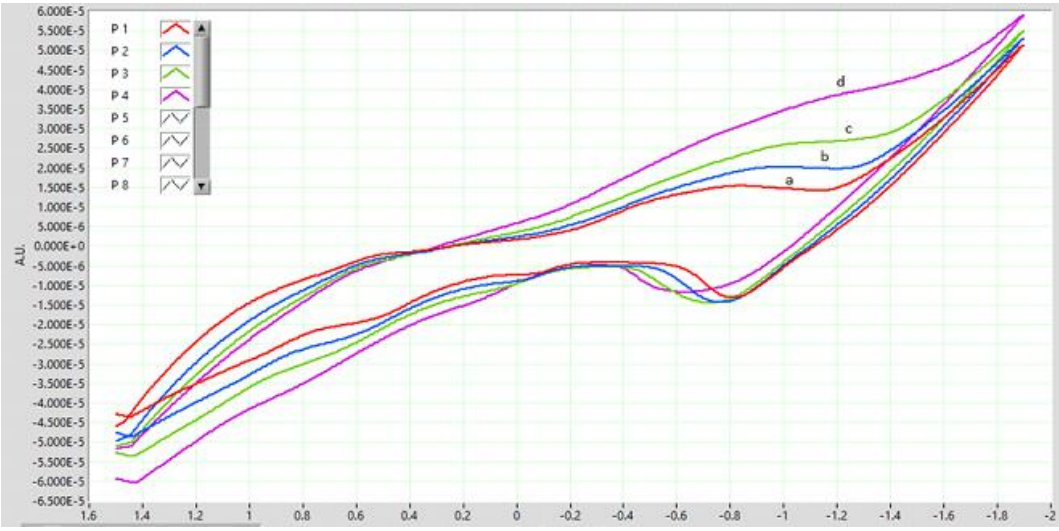

Figure 1: Cyclic voltammogram for PVA-g-SA at scan rates: (a) $0.05 Vs^{-1}$, (b) $0.1\ Vs^{-1}$, (c) $0.2\ Vs^{-1}$, and (d) 0.5 Vs

Table 1: Cyclic voltammogram data of PVA-g-SA at different scan rates

$\nu V.sec^{-1}$	$\nu\ (Vs^{-1})^{1/2}$	Ip_{red1} A (10^{-5})	Fp^{red1} $A/(V.s^{-1})^{1/2}$ (10^{-5})	Ip_{ox1}A (10^{-5})	Fp^{ox1} $A/(V.s^{-1})^{1/2}$ (10^{-5})
0.05	0.223	1.2	5.381166	1.5	6.726457
0.1	0.316	1.3	4.113924	2	6.329114
0.2	0.447	1.5	3.355705	2.5	5.592841
0.5	0.707	1.8	2.545969	3.7	5.23338

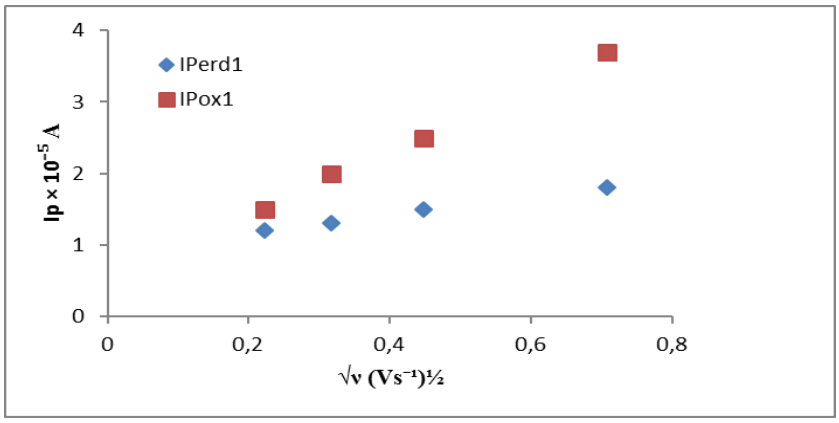

Figure 2: Ip_{red1} and Ip_{ox1} peaks of reduction and oxidation vs. $\nu^{1/2}$ for PVA-g-SA

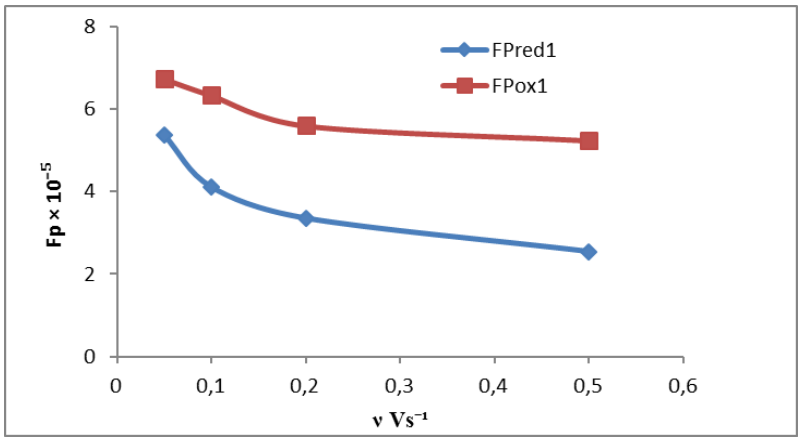

Figure 3: Current function Fp^{red1} and Fp^{ox1} vs. scan rate for PVA-g-SA

Upon doping PVA-g-SA with the dye malachite green, two oxidation peaks and one cathodic peak appeared at the sometime for all doping ratios. It was noticed that the peaks increase in current values as the doping ratios increase. This is probably due to the transfer of electrons from the valence band to the conduction band which causes current growth in value as ν increase [12-13].

Figure 4 shows the cyclic voltammogram of (0.03%) doping of PVA-g-SA at a potential range of 2 to -2V at different scan rates. At scan rate 0.05 Vs^{-1} the ratio exhibited two oxidation peaks, the first oxidation peak appeared at Ep_{ox1}= -0.45V corresponding to anodic peak current Ipox1=1.8 x 10^{-5} A, while the second peak Ep_{ox2} = -1V was corresponded to the anodic peak current $Ip_{ox2}=3\times10^{-5}$ A. At the same scan rate and potential range, the cyclic voltammogram shows also are reduction peak at Ep_{red}= -0.9V with peak cathodic current of $Ip_{red}=1.3\times 10^{-5}$A, and at scan rate of 0.2 Vs^{-1}, 0.5 Vs^{-1}, and 1Vs^{-1}, a new oxidation peak was observed at Ep_{ox}= -0.0.45V with anodic peak current of $Ip_{ox}=(2\text{-}3.5)\times10^{-5}$A shifted to higher values as ν increases. It is obvious that the oxidation potential peaks are shifted to more positive values as ν increases.

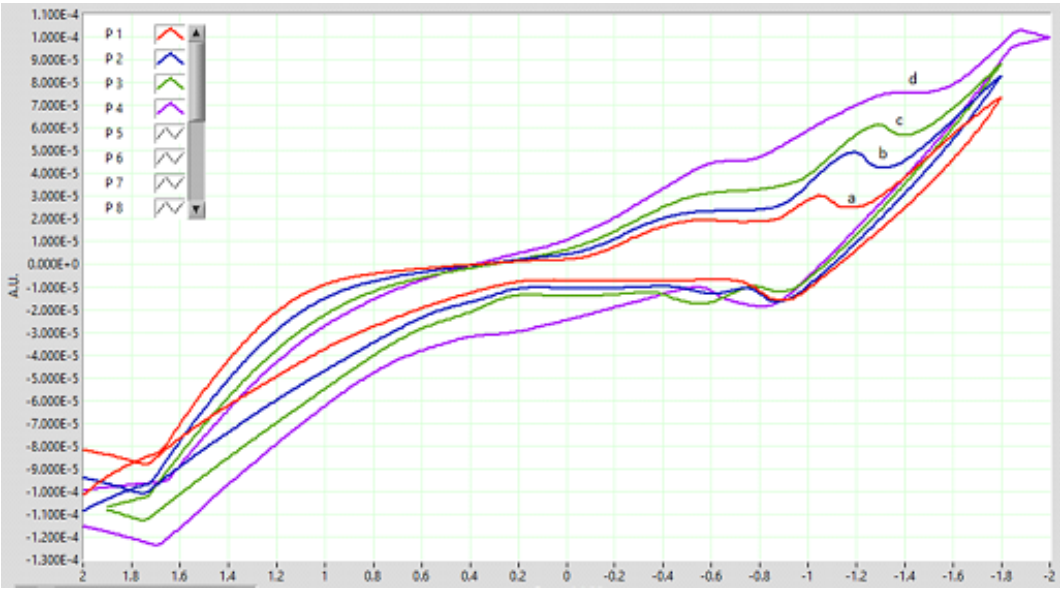

Figure 4: Cyclic voltammogram for 0.03% doping of PVA-g-SA at scan rates: (a) 0.05Vs^{-1}, (b) 0.1 Vs^{-1}, (c) 0.2 Vs^{-1}, and (d) 0.5 Vs^{-1}

The results are presented in Table 2. A linear relationship was obtained between Ip and $\nu^{1/2}$ indicating one electron transfer [14-15], as shown in Figures 5 and 6. While Figures 7 and (8) reveal the relationship between Fp_{ox} vs. ν indicating the same condition Figure 3 for isolation between the primary electron transfer and that of subsequent chemical step.

Table 2: Cyclic voltammogram data of 0.03% doping of PVA-g-SA at different scan rates

$\nu V.sec^{-1}$	$\nu\ (Vs^{-1})^{1/2}$	Ip_{red1} A (10^{-5})	Fp^{red1} $A/(V.s^{-1})^{1/2}$ (10^{-5})	Ip_{ox1}A (10^{-5})	Fp^{ox1} $A/(V.s^{-1})^{1/2}$ (10^{-5})	Ip_{ox2}A (10^{-5})	Fp^{ox2} $A/(V.s^{-1})^{1/2}$ (10^{-5})
0.05	0.223	1.3	5.829596	1.8	8.071749	3	13.45291
0.1	0.316	1.6	5.063291	2	6.329114	3.7	11.70886
0.2	0.447	1.7	3.803132	2.6	5.816555	4.5	10.06711
0.5	0.707	2	2.828854	3.5	4.950495	6.3	8.910891

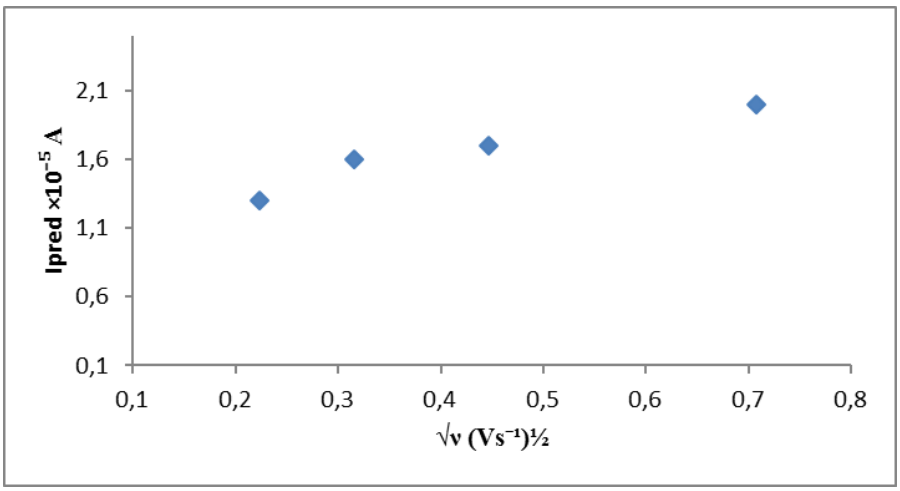

Figure 5: Ipred1 peak of reduction vs. $\nu^{1/2}$ for 0.03% doping of PVA-g-SA

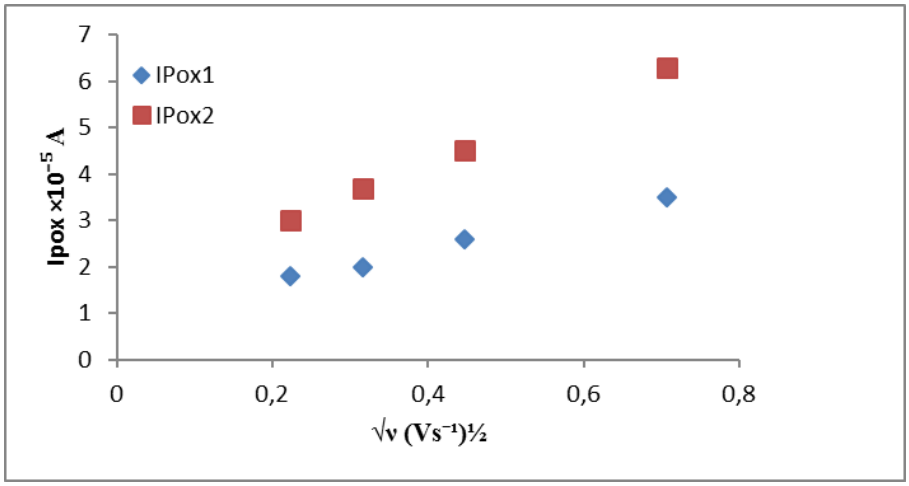

Figure 6: Ip_{ox1} and Ip_{ox2} peaks of oxidation vs. $\nu^{1/2}$ for 0.03% doping of PVA-g-SA

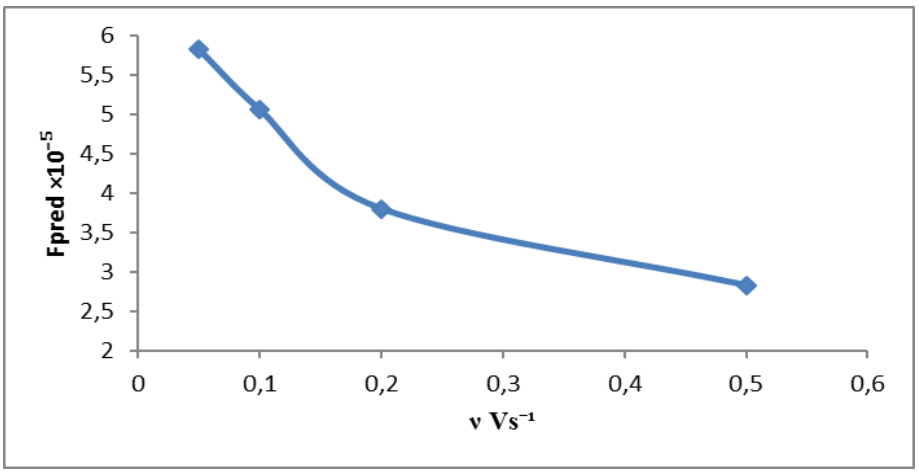

Figure 7: Current function Fp^{red1} vs. scan rate for 0.03% doping of PVA-g-SA

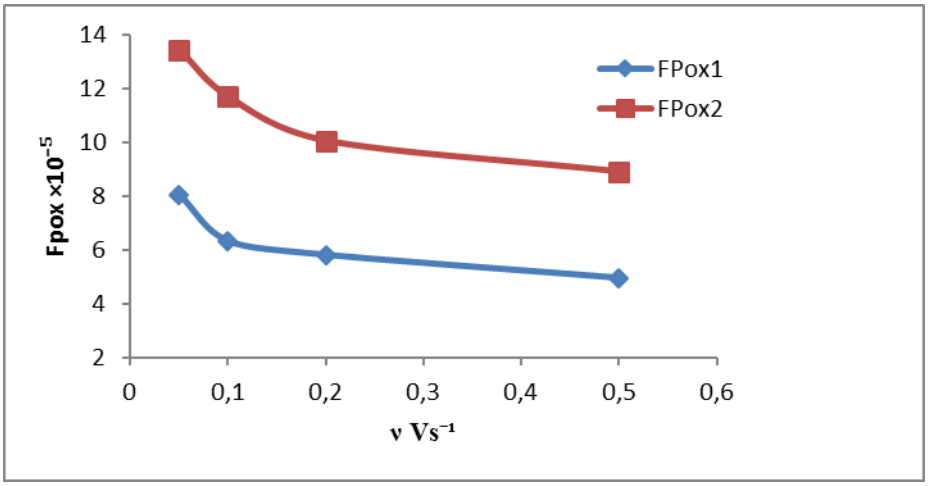

Figure 8: Current function Fp^{ox1} and Fp^{ox2} vs. scan rate for v0.03% doping of PVA-g-SA

The cyclic voltammogram of (0.06%) doping of PVA-g-SA in DMF at scan rate 0.05 Vs^{-1} and potential range from 2 to -2. Figure (9) shows two oxidation peaks at Ep_{ox1}= -0.4V and Ep_{ox2}= -1.2V with peak oxidation current of Ip_{ox1} = 2×10^{-5}A and Ip_{ox2} = 3.3×10^{-5}A, respectively. Also, there is a decreased peak at Ep_{red}= -0.74V with a peak reduction current of Ip_{red} = 2.2×10^{-5}A.

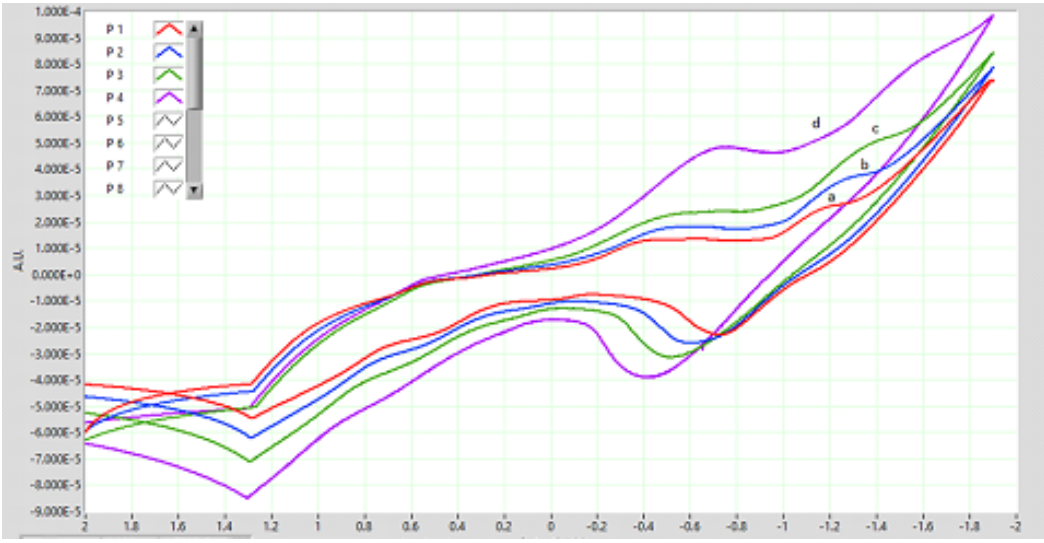

Figure 9: Cyclic voltammogram for 0.06% doping of PVA-g-SA at scan rates: (a) 0.05Vs^{-1}, (b) 0.1 Vs^{-1}, (c) 0.2 Vs^{-1}, and (d) 0.5 Vs^{-1}

As mentioned before, the same trend was obtained at other scan rates, 0.1V^{-1}, 0.2V^{-1}, and 0.5Vs^{-1} a new oxidation peak observed at Ep_{ox}= -0.5V with anodic peak current Ip_{ox}=(2.2-4.2) × 10^{-5}A. The oxidation peaks potential are shifted to more positive values as ν increases, while the reduction peak shifted to higher negative values, as displayed in Figure 9.

The corresponding results were summarized in Table 3, again a linear relationships between both Ip_{red} and Ip_{ox} with $\nu^{1/2}$ were detected, that the electron transfer is a process of one electron as shown in Figures 10 and 11, while Figures 12 and 13 indicate the relationships between Fp with ν for both oxidation and reduction conforming the same characteristics as mentioned before 0.03%.

Table 3: Cyclic voltammogram data of 0.06% doping of PVA-g-SA at different scan rates

νV.sec^{-1}	ν $(Vs^{-1})^{1/2}$	Ip_{red1} A (10^{-5})	Fp^{red1} A/(V.s^{-1})$^{1/2}$ (10^{-5})	Ip_{ox1}A (10^{-5})	Fp^{ox1} A/(V.s^{-1})$^{1/2}$ (10^{-5})	Ip_{ox2}A (10^{-5})	Fp^{ox2} A/(V.s^{-1})$^{1/2}$ (10^{-5})
0.05	0.223	2.2	9.865471	2	8.96861	3.3	14.79821
0.1	0.316	2.4	7.594937	2.2	6.962025	4	12.65823
0.2	0.447	3	6.711409	2.8	6.263982	5	11.18568
0.5	0.707	3.8	5.374823	4.2	5.940594	6.7	9.476662

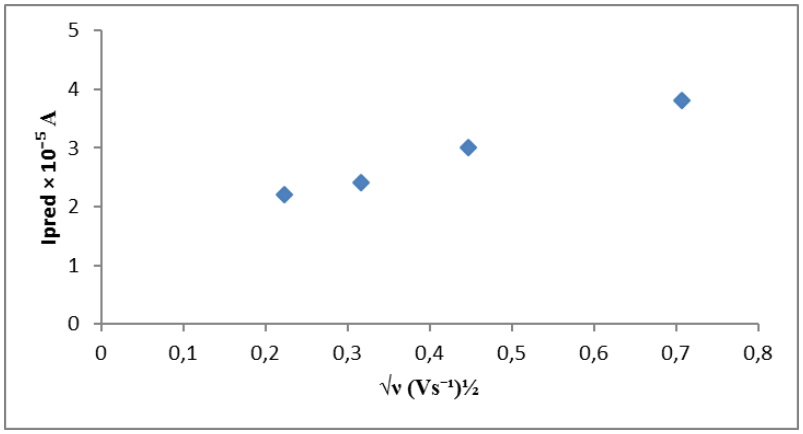

Figure 10: Ipred1 peak of reduction vs. $\nu^{1/2}$ for 0.06% doping of PVA-g-SA

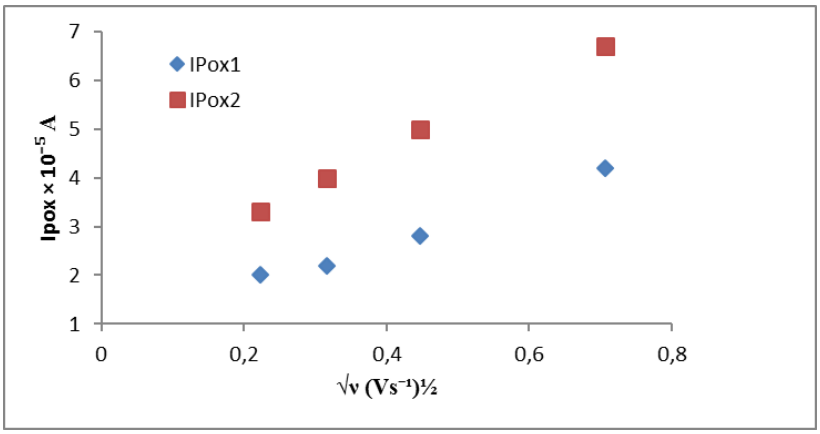

Figure 11: Ip_{ox1} and Ip_{ox2} peaks of oxidation vs. $\nu^{1/2}$ for 0.06% doping of PVA-g-SA

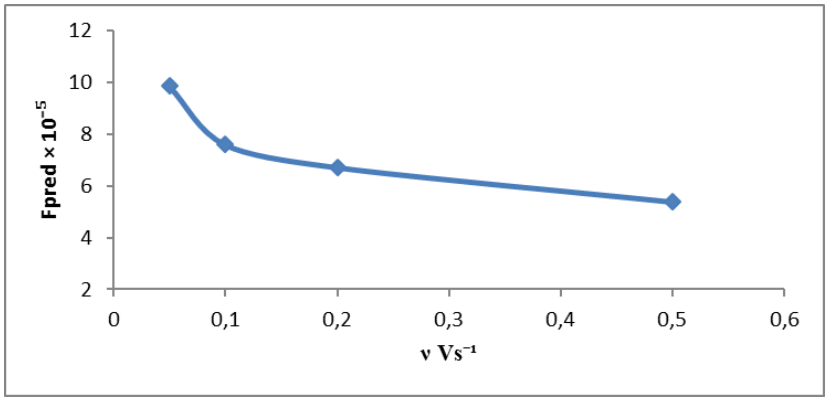

Figure 12: Current function Fp^{red1} vs. scan rate for 0.06% doping of PVA-g-SA

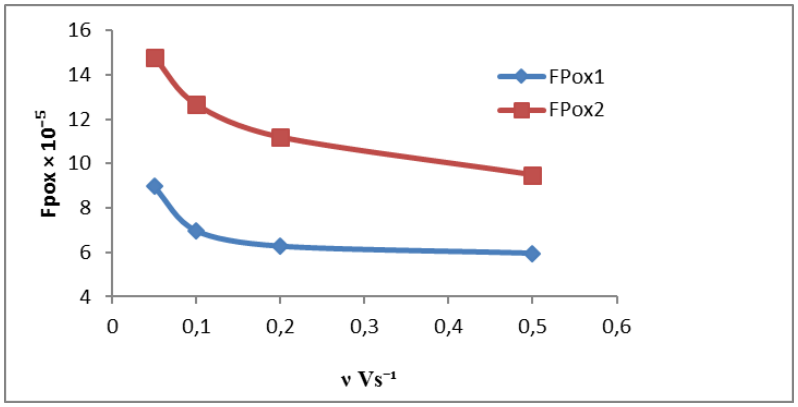

Figure 13: Current function Fp^{ox1} and Fp^{ox2} vs. scan rate for 0.06% doping of PVA-g-SA

Figure 14 displays the cyclic voltammogram of (0.09%) doping of PVA-g-SA at a potential range of 2 to -2Vat different scan rates, while the results of all cyclic voltammogram data are collected in Table 4. It is concluded that as the percentage of doping increases the resultant currents increase gradually indicating more electron transfer occurrence. The cyclic voltammogram of (0.09%) doping of PVA-g-SA in DMF was at scan rate of 0.05 Vs^{-1} and potential range from 2 to -2. There are two oxidation peaks at Ep_{ox1} = -0.6V and Ep_{ox2}= -1.1V with peak oxidation current Ip_{ox1}= 2.4×10^{-5}A and Ip_{ox2} = 3.5×10^{-5}A, respectively. Also, a reduction peak was indicated at Ep_{red}= -0.7 V with a peak reduction current Ip_{red} = 2.5×10^{-5}A.

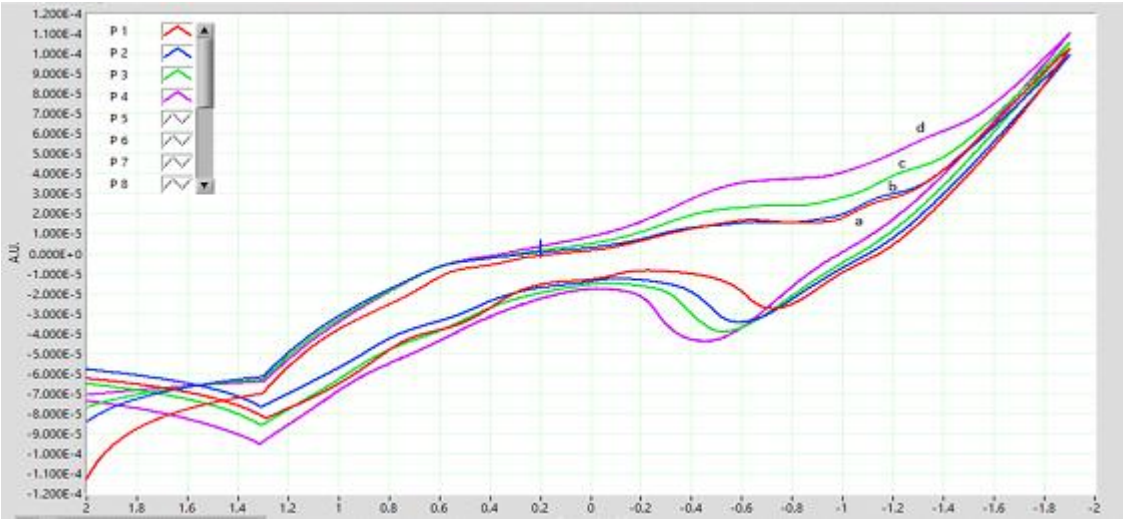

Figure 14: Cyclic voltammogram for 0.09% doping of PVA-g-SA at scan rates: (a) 0.05Vs^{-1}, (b) 0.1 Vs^{-1}, (c) 0.2 Vs^{-1}, and (d) 0.5 Vs^{-1}

As an example, Figures 15 and 16 illustrate once more linear relationships for reduction and oxidation processes giving rise to one electron transfer as well as the same trend exhibited in Figures 17 and 18.

Table 4: Cyclic voltammogram data of 0.09% doping of PVA-g-SA at different scan rates

$\nu V.sec^{-1}$	ν $(Vs^{-1})^{1/2}$	Ip_{red1} A (10^{-5})	Fp^{red1} A/(V.$s^{-1})^{1/2}$ (10^{-5})	Ip_{ox1}A (10^{-5})	Fp^{ox1} A/(V.$s^{-1})^{1/2}$ (10^{-5})	Ip_{ox2}A (10^{-5})	Fp^{ox2} A/(V.$s^{-1})^{1/2}$ (10^{-5})
0.05	0.223	2.5	11.21076	2.4	10.76233	3.5	15.69507
0.1	0.316	3.2	10.12658	2.6	8.227848	4.2	13.29114
0.2	0.447	3.8	8.501119	3	6.711409	5.3	11.85682
0.5	0.707	4.2	5.940594	4.5	6.364922	6.8	9.618105

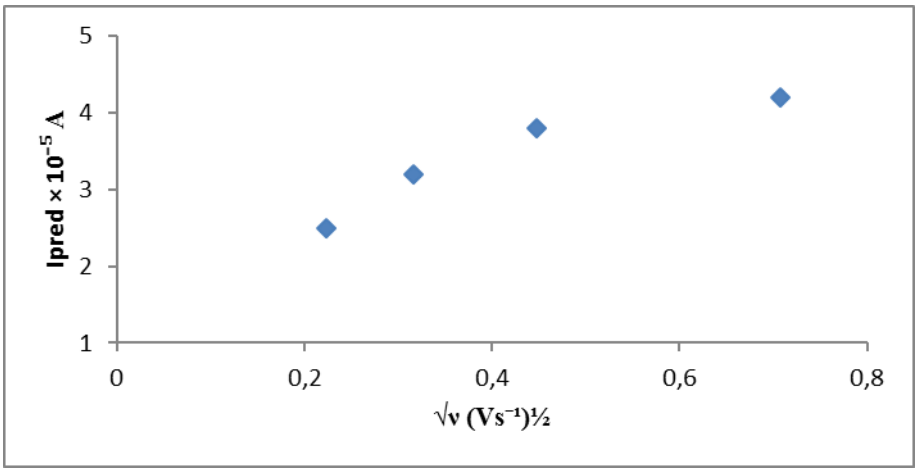

Figure 15: Ipred1 peak of reduction vs. $\nu^{1/2}$ for 0.09% doping of PVA-g-SA

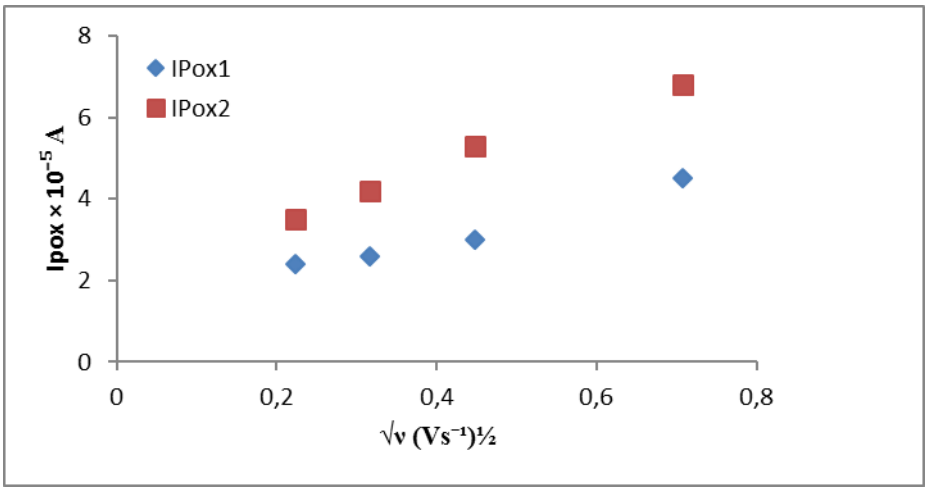

Figure 16: Ip_{ox1} and Ip_{ox2} peaks of oxidation vs. $\nu^{1/2}$ for 0.09% doping of PVA-g-SA

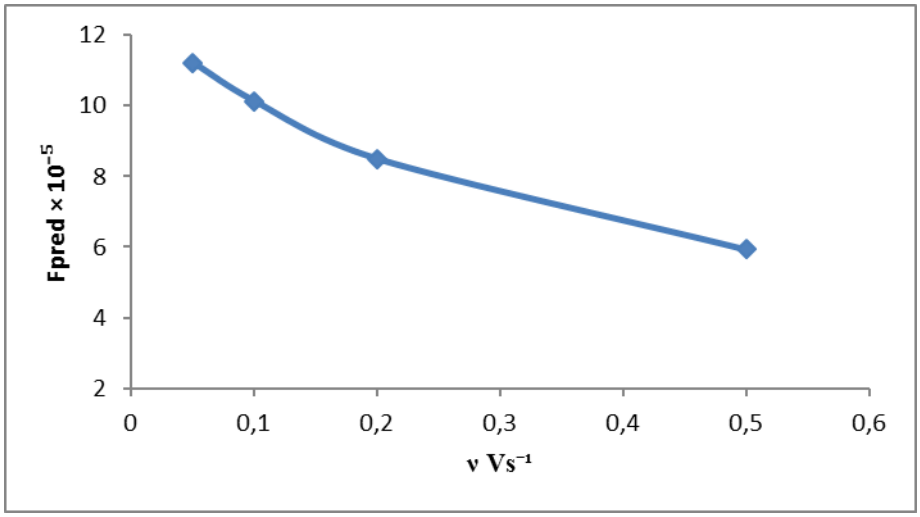

Figure 17: Current function Fp^{red1} vs. scan rate for 0.09% doping of PVA-g-SA

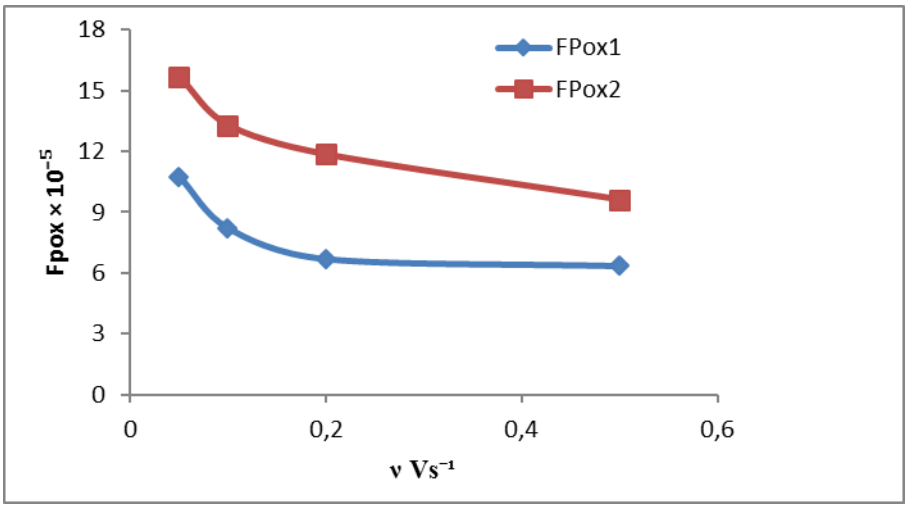

Figure 18: Current function Fp^{ox1} and Fp^{ox2} vs. scan rate for 0.09% doping of PVA-g-SA

In comparison with the preceding percentage, the cyclic voltammogram of (0.12%) doping of PVA-g-SA in DMF at scan rate 0.05 $Vs^{-1}$and potential range from 2 to -2 V indicated two oxidation peaks at Ep_{ox1} = -0.5V and Ep_{ox2}= -1V with peak oxidation current Ip_{ox1} = 2.6×10^{-5}A and Ip_{ox2} = 3.7×10^{-5}A, respectively, as demosntrated in Figure 19. Also, the cyclic voltammogram shows reduction peaks at Ep_{red1}= -0.6V with cathodic peak current Ip_{red} = 2.6×10^{-5}A. The oxidation

peaks are shifted to more positive values, while the reduction peak shifted to higher negative values as ν increases. This is obvious from figure. The main oxidation and reduction peaks increased linearly as the scan rate was increased from 0.1 to 0.5 Vs^{-1} indicating more electron transfer on doping. Table 5 illustrates the results of all cyclic voltammogram data of 0.12% doping of PVA-g-SA.

Figures 20 and 21 illustrate the specific relations between Ip_{red} and Ip_{ox} with $\nu^{1/2}$ characterized linear relationships, which indicate one electron transfer under a controlled diffusion process. Figures 22 and 23 show the same trend as other preceding percentages between Fp^{red} and Fp^{ox} with ν.

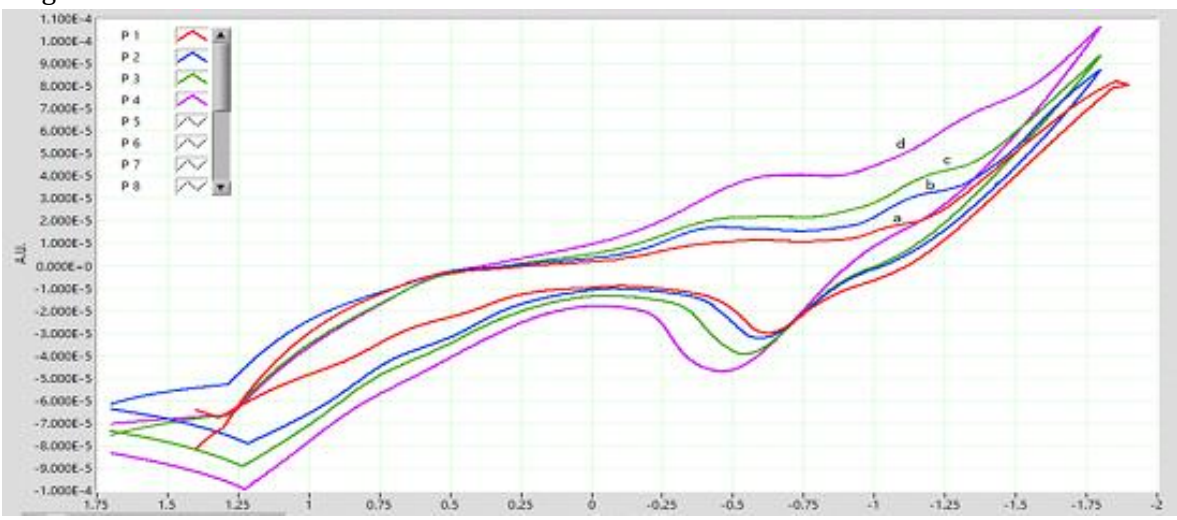

Figure 19: Cyclic voltammogram for 0.12% doping of PVA-g-SA at scan rates: (a) 0.05Vs^{-1}, (b) 0.1 Vs^{-1}, (c) 0.2 Vs^{-1}, and (d) 0.5 Vs^{-1}

Table 5: Cyclic voltammogram data of 0.12% doping of PVA-g-SA at different scan rates

$\nu V.sec^{-1}$	$\nu\ (Vs^{-1})^{1/2}$	Ip_{red1} A (10^{-5})	Fp^{red1} A/(V.s^{-1})$^{1/2}$ (10^{-5})	Ip_{ox1}A (10^{-5})	Fp^{ox1} A/(V.s^{-1})$^{1/2}$ (10^{-5})	Ip_{ox2}A (10^{-5})	Fp^{ox2} A/(V.s^{-1})$^{1/2}$ (10^{-5})
0.05	0.223	2.6	11.65919	2.6	11.65919	3.7	16.59193
0.1	0.316	3	9.493671	2.9	9.177215	4.5	14.24051
0.2	0.447	3.7	8.277405	3.2	7.158837	5.7	12.75168
0.5	0.707	5	7.072136	4.8	6.78925	7	9.90099

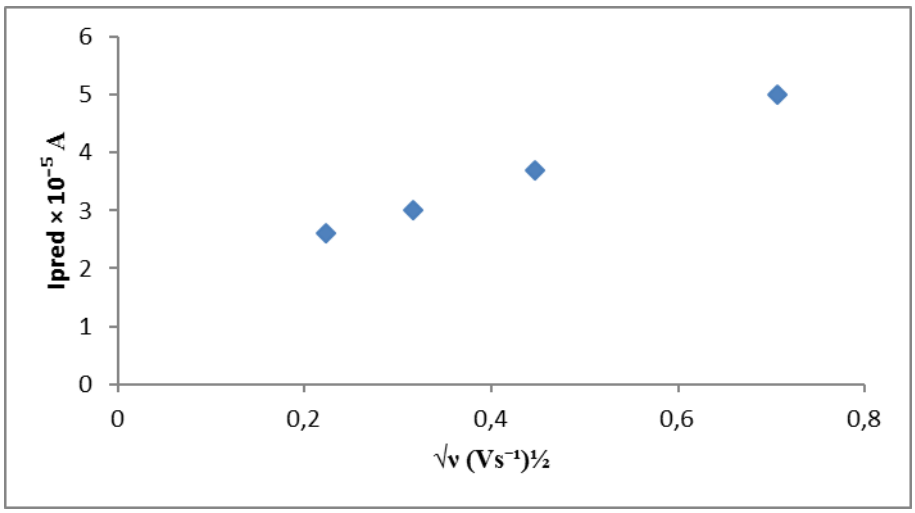

Figure 20: Ipred1 peak of reduction vs. $\nu^{1/2}$ for 0.12% doping of PVA-g-SA

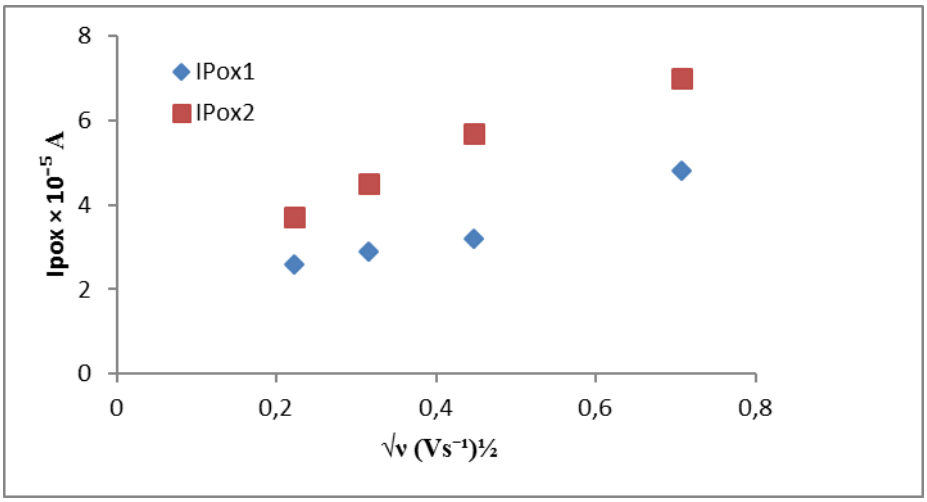

Figure 21: Ip_{ox1} and Ip_{ox2} peaks of oxidation vs. $\nu^{1/2}$ for 0.12% doping of PVA-g-SA

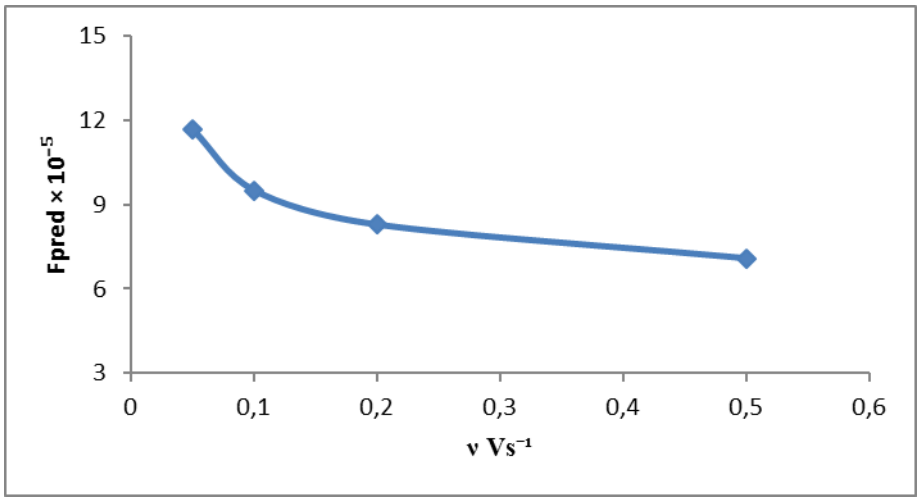

Figure 22: Current function Fp^{red1} vs. scan rate for 0.12% doping of PVA-g-SA

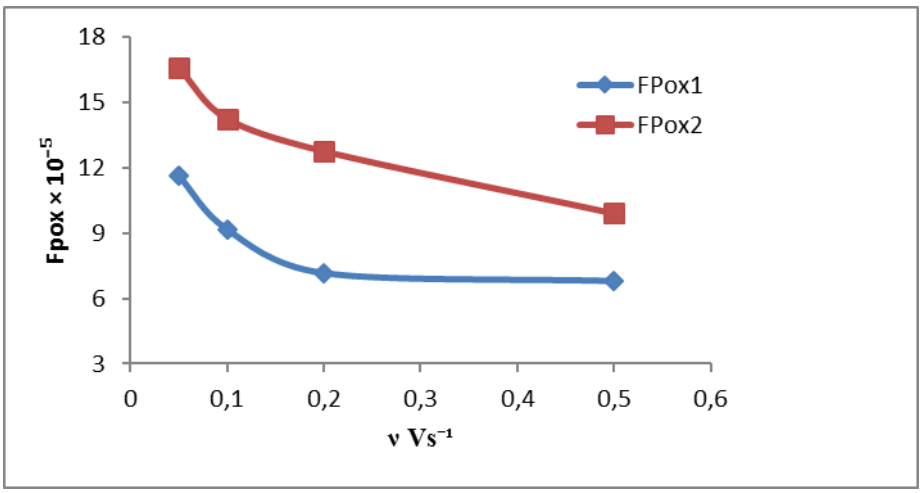

Figure 23: Current function Fp^{ox1} and Fp^{ox2} vs. scan rate for 0.12% doping of PVA-g-SA

The cyclic voltammogram of last percentage (0.15%) doping of PVA-g-SA at a potential range of 2 to -2V at different scan rates show the same behavior as given before, which is abbreviated in Figure 24. All related results are written down in Table 6. Figures 25 and 26 display linear relations between Ip_{red} and Ip_{ox} with $\nu^{1/2}$ which indicate once more one electron transfer under a controlled diffusion process, while Figures 27 and

28 indicate the relations between F^{pred} and F^{pox} with ν.

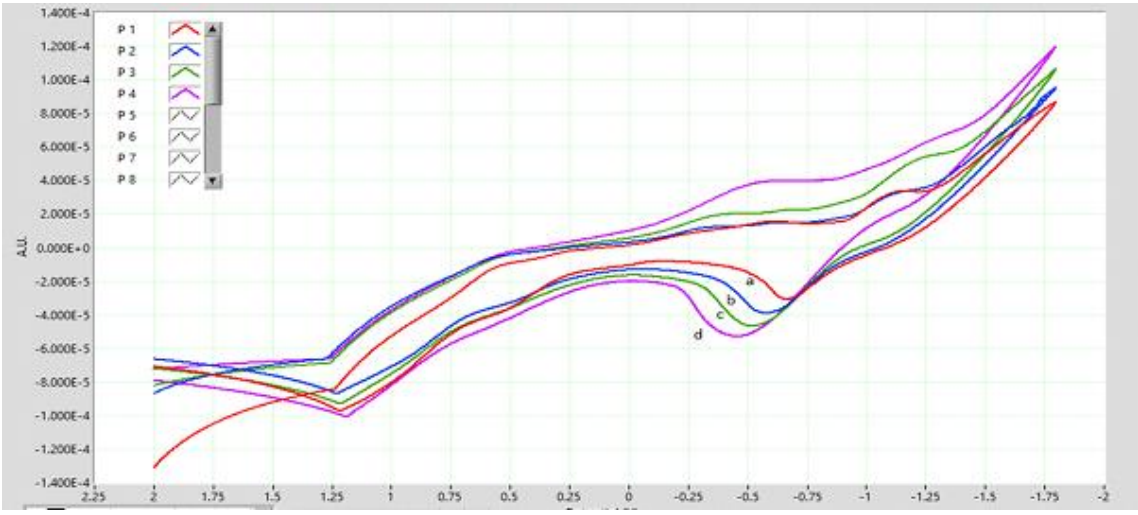

Figure 24: Cyclic voltammogram for 0.15% doping of PVA-g-SA at scan rates: (a) 0.05Vs^{-1}, (b) 0.1 Vs^{-1}, (c) 0.2 Vs^{-1}, and (d) 0.5 Vs^{-1}

Table 5: Cyclic voltammogram data of 0.15% doping of PVA-g-SA at different scan rates

νV.sec^{-1}	ν (Vs^{-1})$^{1/2}$	Ip_{red1} A (10^{-5})	Fp^{red1} A/(V.s^{-1})$^{1/2}$ (10^{-5})	Ip_{ox1}A (10^{-5})	Fp^{ox1} A/(V.s^{-1})$^{1/2}$ (10^{-5})	Ip_{ox2}A (10^{-5})	Fp^{ox2} A/(V.s^{-1})$^{1/2}$ (10^{-5})
0.05	0.223	2.9	13.00448	2.9	13.00448	3.8	17.04036
0.1	0.316	3.6	11.39241	3.3	10.44304	4.9	15.50633
0.2	0.447	4.3	9.619687	4	8.948546	5.8	12.97539
0.5	0.707	5.2	7.355021	5.3	7.496464	7.5	10.6082

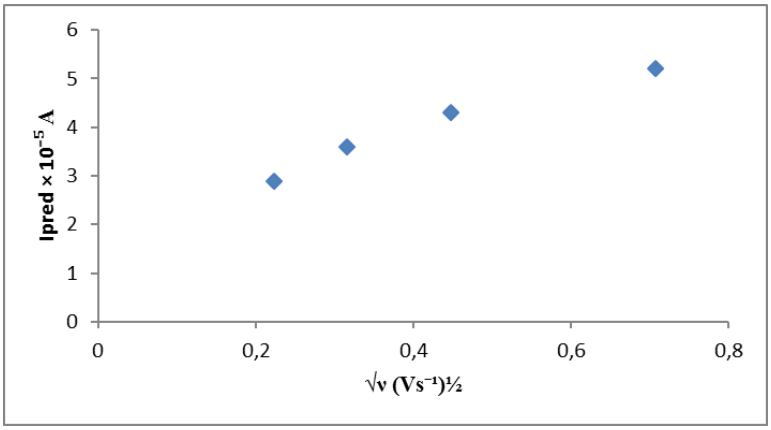

Figure 25: Ipred1 peak of reduction vs. $\nu^{1/2}$ for 0.15% doping of PVA-g-SA

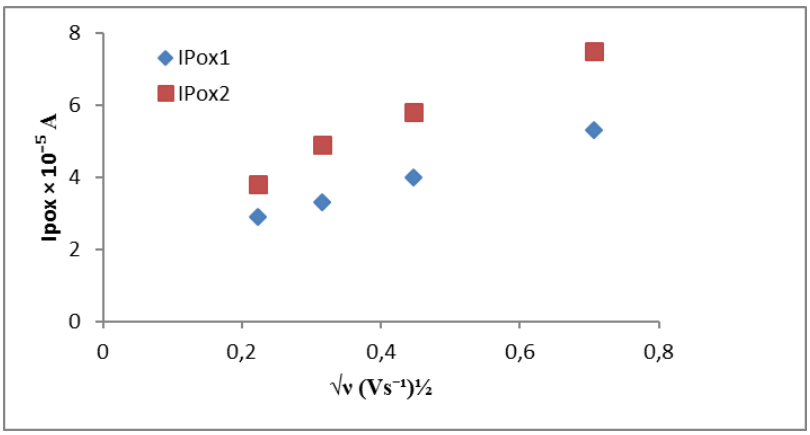

Figure 26: Ip_{ox1} and Ip_{ox2} peaks of oxidation vs. $\nu^{1/2}$ for 0.15% doping of PVA-g-SA

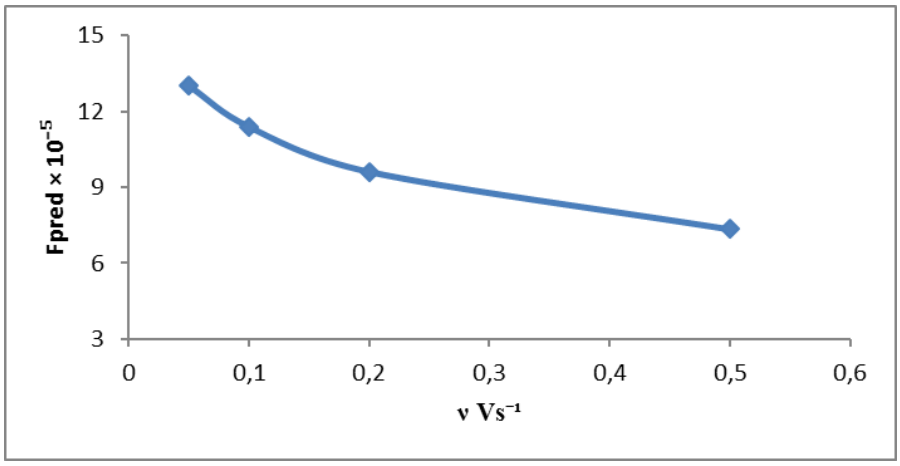

Figure 27: Current function Fp^{red1} vs. scan rate for 0.15% doping of PVA-g-SA

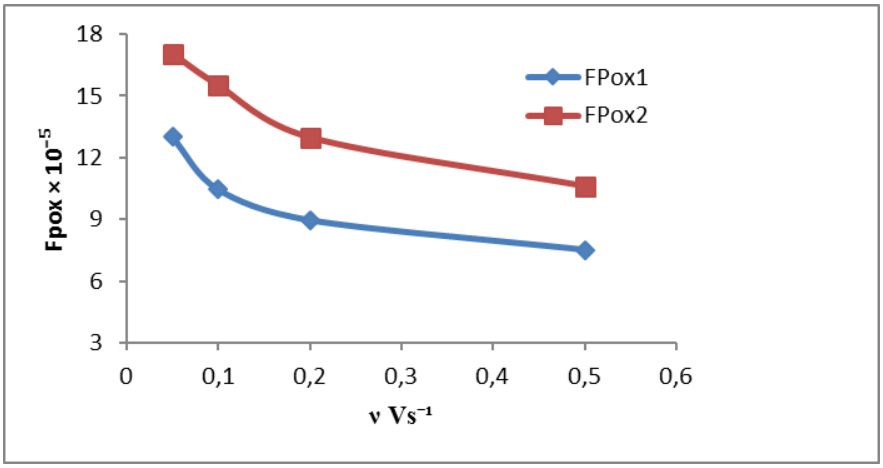

Figure 28: Current function Fp^{ox1} and Fp^{ox2} vs. scan rate for 0.15% doping of PVA-g-SA

Based on comparison, the effect of the different percentages that have been used, it is concluded that 0.15% is the best one among others. Bulk conductivity in doped polymer material is limited by the need for the electrons to jump from one chain to the next, i.e., in molecular terms an intermolecular charge transfer reaction. It is also limited by macroscopic factors such as bad contacts between different crystalline domains in the material [16].

Conclusion

In the study of cyclic voltammetry, the results of a linear relationship between Ip_{red} and I_{pox} with $\nu^{1/2}$ of all doped poly vinyl alcohol-g-succinic acid (PVA-g-SA) with different ratios of malachite green that the electron transfer was a process of one electron transfer.

Acknowledgments

I would like to extend my deep appreciation and sincere thanks to Professor AnisA.AlNajar. The same goes to technical staff at the department of chemistry for providing the necessary technical assistance and support in the experimental.

Funding

This research did not receive any specific grant from fundig agencies in the public, commercial, or not-for-profit sectors.

Authors' contributions

All authors contributed to data analysis, drafting, and revising of the paper and agreed to be responsible for all the aspects of this work.

Conflict of Interest

There are no conflicts of interest in this study.

ORCID:

Samah Hussein Kadhim
https://www.orcid.org/0000-0001-8782-1028

References

[1]. Rountree E.S., McCarthy B.D., Eisenhart T.T., Dempsey J.L., Evaluation of homogeneous electrocatalysts by cyclic voltammetry, *Inorganic chemistry*, 2014, **53**:9983 [Crossref], [Google Scholar], [Publisher]

[2]. Yayla H.G., Peng F., Mangion I.K., McLaughlin M., Campeau L.C., Davies I.W., DiRocco D.A., Knowles R.R., Discovery and mechanistic study of a photocatalytic indoline dehydrogenation for the synthesis of elbasvir, *Chemical science*, 2016, **7**:2066 [Crossref], [Google Scholar], [Publisher]

[3]. Elgrishi N., Rountree K.J., McCarthy B.D., Rountree E.S., Eisenhart T.T., Dempsey L., A practical beginner's guide to cyclic voltammetry, *Journal of chemical education*, 2018, **95**:197 [Crossref], [Google Scholar], [Publisher]

[4]. Arrizabalaga J.H., Simmons A.D., Nollert M.U., Fabrication of an economical Arduino-based uniaxial tensile tester, *J. Chem. Educ.,* 2017, **94**:526 [Crossref], [Google Scholar], [Publisher]

[5]. González-Meza O.A., Larios-Durán E.R., Gutiérrez-Becerra A., Casillas N., Escalante J.I., Bárcena-Soto M., Development of a Randles-Ševčík-like equation to predict the peak current of cyclic voltammetry for solid metal hexacyanoferrates, *Journal of Solid State Electrochemistry*, 2019, **23**:3123 [Crossref], [Google Scholar], [Publisher]

[6]. Wang Y., Laborda E., Compton R.G., Electrochemical oxidation of nitrite: Kinetic, mechanistic and analytical study by square wave voltammetry, *Journal of Electroanalytical Chemistry*, 2012, **670**:56 [Crossref], [Google Scholar], [Publisher]

[7]. Elgrishi N., McCarthy B.D., Rountree E.S., Dempsey J.L., Reaction pathways of hydrogen-evolving electrocatalysts: Electrochemical and spectroscopic studies of proton-coupled electron transfer processes, *ACS Catalysis*, 2016, **6**:3644 [Crossref], [Google Scholar], [Publisher]

[8]. Murhekar G.H., Synthesis and Characterization of Complexes of Remodulated Polyvinyl Alcohol Conjugates, *International Journal of Advanced Research in Chemical Science*, 2017, **4**:32 [Crossref], [Google Scholar], [Publisher]

[9]. Hossain M.M., Tanmyc T.T., A Novel Approach for Total Synthesis of Stemona Alkaloid: Tuberostemonamide. *Journal of Applied Organometallic Chemistry,* 2021, **1**: 159 [Crossref], [Publisher]

[10]. Costentin C., Savéant J.M., Multielectron, multistep molecular catalysis of electrochemical reactions: Benchmarking of homogeneous catalysts, *ChemElectroChem*, 2014, 1, 1226– 1236, [Crossref], [Google Scholar], [Publisher]

[11]. Luo J., Hu B., Sam A., Liu T.L., Metal-free electrocatalytic aerobic hydroxylation of arylboronic acids, *Organic letters*, 2018, **20**:361 [Crossref], [Google Scholar], [Publisher]

[12]. Sasikumar R., Manisankar P., Electrochemically synthesized nano size copolymer, poly (aniline-co-ethyl 4-aminobenzoate) and its spectroelectrochemical studies, *Polymer*, 2011, **52**:3710 [Crossref], [Google Scholar], [Publisher]

[13]. Jackson M.N., Surendranath Y., Molecular control of heterogeneous electrocatalysis through graphite conjugation, *Accounts of Chemical Research*, 2019, **52**:3432 [Crossref], [Google Scholar], [Publisher]

[14]. Lee J., Muya J.T., Chung H., Chang J., Unraveling V (V)-V (IV)-V (III)-V (II) redox electrochemistry in highly concentrated mixed acidic media for a vanadium redox flow battery: origin of the parasitic hydrogen evolution reaction, *ACS applied materials & interfaces*, 2019, **11**:42066 [Crossref], [Google Scholar], [Publisher]

[15]. Sandford C., Edwards M.A., Klunder K.J., Hickey D.P., Li M., Barman K., Sigman M.S., White H.S., Minteer S.D., A synthetic chemist's guide to electroanalytical tools for studying reaction mechanisms, *Chemical science*, 2019, **10**:6404 [Crossref], [Google Scholar], [Publisher]

[16]. Bediako D.K., Surendranath Y., Nocera D.G., Mechanistic studies of the oxygen evolution reaction mediated by a nickel–borate thin film electrocatalyst, *Journal of the American Chemical Society*, 2013, **135**:3662 [Crossref], [Google Scholar], [Publisher]

HOW TO CITE THIS ARTICLE
Samah Hussein Kadhim, Electrochemical Investigation of Poly Vinyl Alcohol -G- Succinic Acid Doped with Malachite Green. *J. Med. Chem. Sci.*, 2022, 5(7) 1265-1280
https://doi.org/10.26655/JMCHEMSCI.2022.7.16
URL: http://www.jmchemsci.com/article_154650.html